Woven, Polycatenated, or Cage Structures: Effect of Modulation of Ligand Curvature in Heteroleptic Uranyl Ion Complexes

Sotaro Kusumoto, Youssef Atoini, Shunya Masuda, Yoshihiro Koide, Kittipong Chainok, Yang Kim, Jack Harrowfield, Pierre Thuéry

Woven, Polycatenated or Cage Structures: Effect of Modulation of Ligand Curvature in Heteroleptic Uranyl Ion Complexes

Sotaro Kusumoto,[a] Youssef Atoini,[b] Shunya Masuda,[a] Yoshihiro Koide,[a] Kittipong Chainok,*[,c] Yang Kim,*[,c,d] Jack Harrowfield,*[,e] and Pierre Thuéry*[,f]

[a] Department of Material & Life Chemistry, Kanagawa University, 3-27-1 Rokkakubashi, Kanagawa-ku, Yokohama 221-8686, Japan

[b] Technical University of Munich, Campus Straubing, Schulgasse 22, 94315 Straubing, Germany

[c] Thammasat University Research Unit in Multifunctional Crystalline Materials and Applications (TU-MCMA), Faculty of Science and Technology, Thammasat University, Pathum Thani 12121, Thailand

[d] Department of Chemistry, Graduate School of Science and Technology, Institute of Industrial Nanomaterials (IINa), Kumamoto University, 2-39-1 Kurokami, Chuo-ku, Kumamoto 860-8555, Japan

[e] Université de Strasbourg, ISIS, 8 allée Gaspard Monge, 67083 Strasbourg, France

[f] Université Paris-Saclay, CEA, CNRS, NIMBE, 91191 Gif-sur-Yvette, France

ABSTRACT: Combining the flexible zwitterionic dicarboxylate 4,4′-bis(2-carboxylatoethyl)-4,4′-bipyridinium (L) and the anionic dicarboxylate ligands isophthalate ($ipht^{2-}$) and 1,2-, 1,3- or 1,4-phenylenediacetate (1,2-, 1,3- and 1,4-pda^{2-}), of varying shape and curvature, has allowed isolation of five uranyl ion complexes by synthesis under solvo-hydrothermal conditions. $[(UO_2)_2(L)(ipht)_2]$ (**1**) and $[(UO_2)_2(L)(1,2\text{-pda})_2]\cdot 2H_2O$ (**2**) have the same stoichiometry and both crystallize as monoperiodic coordination polymers containing two uranyl–(anionic carboxylate) strands united by L linkers into a wide ribbon, all ligands being in the divergent conformation. Complex **3**, $[(UO_2)_2(L)(1,3\text{-pda})_2]\cdot 0.5CH_3CN$, with the same stoichiometry but ligands in a convergent conformation, is a discrete, binuclear species which is the first example of a heteroleptic uranyl carboxylate coordination cage. With all ligands in a divergent conformation, $[(UO_2)_2(L)(1,4\text{-pda})(1,4\text{-pdaH})_2]$ (**4**) crystallizes as a sinuous and thread-like monoperiodic polymer; two families of chains run along different directions and are woven into diperiodic layers. Modification of the synthetic conditions leads to $[(UO_2)_4(LH)_2(1,4\text{-pda})_5]\cdot H_2O\cdot 2CH_3CN$ (**5**), a monoperiodic polymer based on tetranuclear $(UO_2)_4(1,4\text{-pda})_4$ rings; intrachain hydrogen bonding of the terminal LH^+ ligands results in diperiodic network formation through parallel polycatenation involving the tetranuclear rings and the LH^+ rods. Complexes **1**–**3** and **5** are emissive, with complex **2** having the highest photoluminescence quantum yield (19%), and their spectra show the maxima positions usual for tris-κ^2O,O'-chelated uranyl cations.

INTRODUCTION

Heteroleptic metal–organic cages have aroused much interest recently for their possible applications in catalysis and multiple other areas requiring selective guest inclusion, taking advantage of the possibility they offer of easily introducing multifunctionality.[1] Besides more sophisticated synthetic approaches, the easiest pathway toward such cages is through integrative self-sorting[2] from a mixture of ligands and unprotected metal cations, with charge separation being a particularly appealing strategy.[3] A number of uranyl-based cages or clusters have now been described[4–27] and, although some of them include both peroxide and carboxylate,[4,6,9] phosphonate,[14,25] phosphate[7,15,18] or carboxyphosphonate[20] ligands, all others are homoleptic. In particular, no example is known of a cage involving different polycarboxylate donors. In the course of an investigation of mixed-ligand uranyl ion complexes with combinations of zwitterionic and anionic polycarboxylates, we recently reported the synthesis of three heteroleptic ring-shaped complexes involving the zwitterionic/anionic carboxylate couples Ni(tpyc)$_2$/*cis*-1,2-cyclohexanedicarboxylate or 2,5-thiophenedicarboxylate (tpyc$^-$ = 2,2′;6′,2″-terpyridine-4′-carboxylate)[28] or 1,1′-[(2,3,5,6-tetramethylbenzene-1,4-diyl)bis(methylene)]bis(pyridin-1-ium-4-carboxylate)/1,2,3,4-cyclobutanetetracarboxylate,[29] which results led us to contemplate the possible formation of mixed-ligand cages. Of further interest, the elongated and flexible zwitterions *N,N,N′,N′*-tetramethylethane-1,2-diammonioacetate and *N,N,N′,N′*-tetramethylpropane-1,3-diammonioacetate have recently been shown to be conducive to the formation of entangled networks.[30]

In using the zwitterionic dicarboxylate ligand 4,4′-bis(2-carboxylatoethyl)-4,4′-bipyridinium (L), shown in Scheme 1, different to those of the previous studies, we have now isolated five uranyl ion complexes containing as coligands either isophthalate (ipht^{2-}), 1,2-phenylenediacetate (1,2-pda^{2-}), 1,3-phenylenediacetate (1,3-pda^{2-}), or 1,4-phenylenediacetate (1,4-pda^{2-}), all obtained under solvo-hydrothermal conditions, and determined their crystal

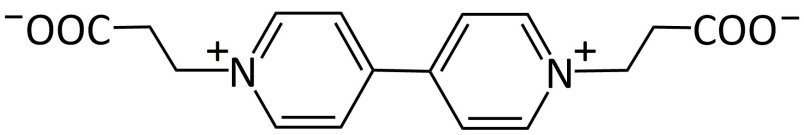

Scheme 1. The Zwitterionic Carboxylate Ligand L

structure. The zwitterion L has seldom been used in coordination chemistry, but it is notable that coordination polymers formed with Zn^{II} and Cd^{II} include also isophthalate ligands,[31,32] while a related bipyridinium-based zwitterion has previously been used to complex uranyl ions in combination with phthalate or terephthalate ligands.[33] With proper choice of the anionic coligand, uranyl complexation by the ligand L has now enabled isolation of the first heteroleptic uranyl polycarboxylate coordination cage and also of a complex which is, to the best of our knowledge, a unique example of woven chains in uranyl chemistry, this topology having recently attracted considerable interest.[34–40]

EXPERIMENTAL SECTION

Syntheses. ***Caution!*** *Uranium is a radioactive and chemically toxic element, and uranium-containing samples must be handled with suitable care and protection. Small quantities of reagents and solvents were employed to minimize any potential hazards arising both from the presence of uranium and the use of pressurized vessels for the syntheses.*

$[UO_2(NO_3)_2(H_2O)_2]\cdot 4H_2O$ (RP Normapur, 99%) was purchased from Prolabo, and the carboxylic acids were from Aldrich. *N,N,N′,N′*-Tetramethylpropane-1,3-diammonioacetate hydrochloride was prepared as previously reported.[30] The ^1H NMR spectrum of LH_2Cl_2 was recorded on a JEOL 400 MHz spectrometer. Elemental analyses of the uranyl ion complexes were performed by MEDAC Ltd.

LH_2Cl_2. LH_2Cl_2 was prepared by a slight modification of the previously reported method.[41] 4,4′-Bipyridine (15 mmol) and acrylic acid (30 mL, 50-fold molar excess) were dissolved in chloroform (20 mL) and stirred at ambient temperature for 1 d. Acetone/c-HCl (6:1 v/v, 12 mL) mixed solvent was then added to the reaction mixture. The resulting pale-yellow precipitate was filtered off and recrystallized from methanol-acetone (1:1 v/v) to give a hygroscopic powder. Yield, 3.0 g. Elemental analysis of the ligand was not performed due to its hygroscopicity. ^{1}H NMR (400 MHz, D_2O): δ = 3.56 (t, 4H), 4.86 (t, 4H), 8.40 (d, 4H), 9.06 (d, 4H) (Figure S1).

$[(UO_2)_2(L)(ipht)_2]$ (1). LH_2Cl_2 (19 mg, 0.05 mmol), isophthalic acid (9 mg, 0.05 mmol), $[UO_2(NO_3)_2(H_2O)_2]\cdot 4H_2O$ (25 mg, 0.05 mmol), acetonitrile (0.2 mL), and demineralized water (0.6 mL) were placed in a 15 mL tightly closed glass vessel and heated at 140 °C under autogenous pressure, giving a few light yellow crystals of compound **1** within three weeks.

$[(UO_2)_2(L)(1,2\text{-}pda)_2]\cdot 2H_2O$ (2). LH_2Cl_2 (19 mg, 0.05 mmol), 1,2-phenylenediacetic acid (10 mg, 0.05 mmol), $[UO_2(NO_3)_2(H_2O)_2]\cdot 4H_2O$ (25 mg, 0.05 mmol), acetonitrile (0.2 mL), and demineralized water (0.6 mL) were placed in a 15 mL tightly closed glass vessel and heated at 140 °C under autogenous pressure, giving light yellow crystals of compound **2** overnight (19 mg, 60% yield). Anal. calcd for $C_{36}H_{36}N_2O_{18}U_2$: C, 34.30; H, 2.88; N, 2.22. Found: C, 34.29; H, 3.06; N, 2.25%.

$[(UO_2)_2(L)(1,3\text{-}pda)_2]\cdot 0.5CH_3CN$ (3). LH_2Cl_2 (19 mg, 0.05 mmol), 1,3-phenylenediacetic acid (10 mg, 0.05 mmol), $[UO_2(NO_3)_2(H_2O)_2]\cdot 4H_2O$ (25 mg, 0.05 mmol), acetonitrile (0.2 mL), and demineralized water (0.6 mL) were placed in a 15 mL tightly closed glass vessel and heated at 140 °C under autogenous pressure, giving light yellow crystals of compound **3** within two weeks (16 mg, 51% yield). The elemental analysis indicates the presence of two additional water molecules, in agreement with the presence of voids containing

disordered solvent molecules in the structure (see below). Anal. calcd for $C_{37}H_{33.5}N_{2.5}O_{16}U_2$ + $2H_2O$: C, 34.69; H, 2.95; N, 2.73. Found: C, 34.55; H, 2.79; N, 2.67%.

$[(UO_2)_2(L)(1,4\text{-pda})(1,4\text{-pdaH})_2]$ (4). LH_2Cl_2 (19 mg, 0.05 mmol), 1,4-phenylenediacetic acid (10 mg, 0.05 mmol), $[UO_2(NO_3)_2(H_2O)_2]\cdot 4H_2O$ (25 mg, 0.05 mmol), acetonitrile (0.2 mL), and demineralized water (0.6 mL) were placed in a 15 mL tightly closed glass vessel and heated at 140 °C under autogenous pressure, giving light yellow crystals of compound **4** within ten days (19 mg, 80% yield). The elemental analysis indicates the presence of three additional water molecules, in keeping with the presence of voids containing disordered solvent molecules in the structure (see below), although the number of water molecules determined from elemental analysis is larger than that estimated from the structure determination, possibly indicating the slightly hygroscopic nature of the sample. Anal. calcd for $C_{46}H_{42}N_2O_{20}U_2$ + $3H_2O$: C, 37.51; H, 3.28; N, 1.90. Found: C, 37.40; H, 3.16; N, 2.06%.

$[(UO_2)_4(LH)_2(1,4\text{-pda})_5]\cdot H_2O\cdot 2CH_3CN$ (5). LH_2Cl_2 (19 mg, 0.05 mmol), *N,N,N′,N′*-tetramethylpropane-1,3-diammonioacetate hydrochloride (16 mg, 0.05 mmol) 1,4-phenylenediacetic acid (20 mg, 0.10 mmol), $[UO_2(NO_3)_2(H_2O)_2]\cdot 4H_2O$ (50 mg, 0.10 mmol), acetonitrile (0.2 mL), and demineralized water (0.6 mL) were placed in a 15 mL tightly closed glass vessel and heated at 140 °C under autogenous pressure, giving a few light yellow crystals of compound **5** within ten days.

Crystallography. The data were collected at 100(2) K on a Bruker D8 Quest diffractometer equipped with an Incoatec microfocus source (IμS 3.0 Mo, λ = 0.71073 Å) and a PHOTON III area detector, and operated through the APEX3 software.[42] The crystals were mounted on Mitegen micromounts with a protective coating of Paratone-N oil (Hampton Research). The data were processed with SAINT[43] and empirical absorption corrections (multi-scan) were made with SADABS.[44,45] All structures were solved by intrinsic phasing with SHELXT,[46] and refined by full-matrix least-squares on F^2 with SHELXL,[47] using the ShelXle

interface.[48] All non-hydrogen atoms were refined with anisotropic displacement parameters. The hydrogen atoms bound to oxygen atoms in **2** and **5** were found and refined with restraints on bond lengths and angles, and with an isotropic displacement parameter equal to 1.2 (carboxylic group) or 1.5 times (water) that of the attached atom. All other hydrogen atoms were introduced at calculated positions and were treated as riding atoms with an isotropic displacement parameter equal to 1.2 times that of the parent atom (1.5 for CH_3). The nitrogen atom of the acetonitrile molecule in **3** is close to its image by symmetry and this molecule has been given an occupancy parameter of 0.5 accordingly. Some voids in the structures of **3** and **4** contain disordered and badly resolved water solvent molecules and the SQUEEZE software[49] was used to subtract their contribution to the structure factors. About 22 and 14 electrons per asymmetric unit were found in the voids in **3** and **4**, respectively, corresponding to about 2 or 1 water molecules, which matches the presence of two water molecules deduced from the elemental analysis of **3**, whereas there is some discrepancy in the case of **4** (see above). The molecular plots were drawn with ORTEP-3,[50,51] and the polyhedral representations with VESTA.[52] The topological analyses were made with ToposPro.[53] The Kitaigorodski packing indexes were evaluated with PLATON.[54] Crystal data and refinement details are given in Table 1.

The Hirshfeld surface[55] of **3** was calculated with CrystalExplorer.[56] It should be noted that it is necessarily approximate due to the presence of unresolved solvent molecules and the disorder affecting the acetonitrile molecule; however, this should not prevent in any notable way the surface to correctly show the cage···cage interactions.

Luminescence Measurements. Emission spectra were recorded on solid samples using an Edinburgh Instruments FS5 spectrofluorimeter equipped with a 150 W CW ozone-free xenon arc lamp, dual-grating excitation and emission monochromators (2.1 nm mm^{-1} dispersion; 1200 grooves mm^{-1}) and an R928P photomultiplier detector. The powdered compounds were pressed

to the wall of a quartz tube, and the measurements were performed using the right-angle mode in the SC-05 cassette. An excitation wavelength of 420 nm was used in all cases and the emission was monitored between 450 and 600 nm. The quantum yield measurements were performed by using a Hamamatsu Quantaurus C11347 absolute photoluminescence quantum yield spectrometer and exciting the samples between 300 and 400 nm.

Table 1. Crystal Data and Structure Refinement Details

	1	**2**	**3**	**4**	**5**
chemical formula	$C_{32}H_{24}N_2O_{16}U_2$	$C_{36}H_{36}N_2O_{18}U_2$	$C_{37}H_{33.5}N_{2.5}O_{16}U_2$	$C_{46}H_{42}N_2O_{20}U_2$	$C_{86}H_{82}N_6O_{37}U_4$
M (g mol^{-1})	1168.60	1260.73	1245.22	1418.87	2743.69
cryst syst	triclinic	triclinic	monoclinic	monoclinic	monoclinic
space group	$P\bar{1}$	$P\bar{1}$	$P2/n$	$C2/c$	$P2_1/c$
a (Å)	9.2054(3)	8.0138(2)	21.8262(6)	34.5364(16)	15.7263(11)
b (Å)	9.8665(3)	10.0044(3)	9.7656(3)	8.0673(3)	11.2939(8)
c (Å)	9.8834(4)	12.0834(3)	22.1896(6)	17.7359(8)	25.4533(14)
α (deg)	80.0331(15)	86.9110(11)	90	90	90
β (deg)	83.0380(15)	86.8458(12)	118.4684(12)	108.375(2)	100.456(3)
γ (deg)	67.6884(14)	74.7875(11)	90	90	90
V (Å^3)	816.40(5)	932.62(4)	4157.7(2)	4689.5(4)	4445.7(5)
Z	1	1	4	4	2
reflns collcd	62890	41890	37746	57832	78767
indep reflns	4966	5707	7888	4438	8442
obsd reflns [$I > 2\sigma(I)$]	4832	5381	6213	4003	7567
R_{int}	0.041	0.056	0.072	0.061	0.076
params refined	235	268	533	319	614
R_1	0.014	0.021	0.038	0.030	0.034
wR_2	0.035	0.045	0.093	0.078	0.082
S	1.118	1.084	1.044	1.092	1.221
$\Delta\rho_{min}$ (e Å^{-3})	–0.84	–1.91	–1.42	–1.31	–1.52
$\Delta\rho_{max}$ (e Å^{-3})	1.29	1.70	2.92	2.17	1.60

RESULTS AND DISCUSSION

Crystal Structures. While all four syntheses employed well-established solvothermal procedures and provided the desired mixed-ligand complexes, it is worthy of note that in no case was chloride ion derived from the zwitterionic ligand precursor found in the products. Chloride is a good ligand for uranyl ion and its presence in reaction mixtures can lead to complications for carboxylate complex syntheses.[30] The unique uranium atom in $[(UO_2)_2(L)(ipht)_2]$ (**1**) is tris-κ^2O,O'-chelated by three carboxylate groups, two from $ipht^{2-}$ and

one from the centrosymmetric L [U–O(oxo), 1.7681(15) and 1.7847(14) Å; U–O(carboxylato), 2.4491(14)–2.4802(15) Å] (Figure 1). The $ipht^{2-}$ anion is nearly planar [dihedral angles between the carboxylate groups and the ring, 7.3(3) and 15.1(2)°], while L is kinked at both

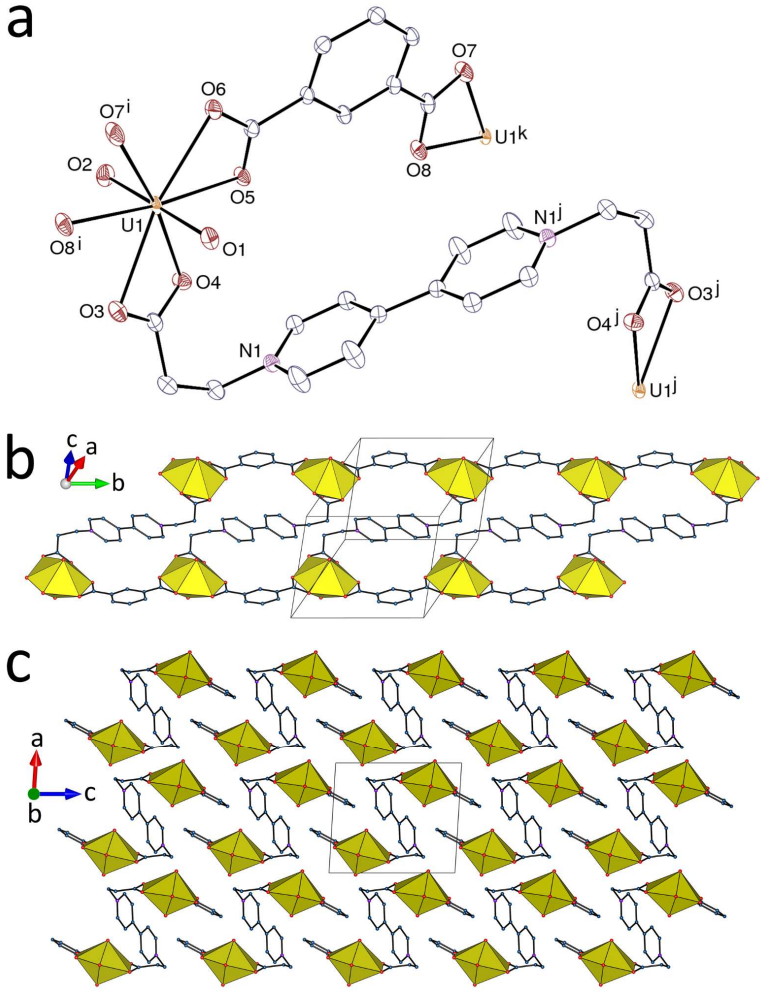

Figure 1. (a) View of compound **1**. Displacement ellipsoids are drawn at the 50% probability level and hydrogen atoms are omitted. Symmetry codes: i = x, y + 1, z; j = 1 – x, 1 – y, 1 – z; k = x, y – 1, z. (b) View of one chain. (c) Packing with chains viewed end-on.

ends and thus adopts a divergent S-shape with the carboxylate groups lying in parallel planes nearly orthogonal to that of the planar bipyridine unit. The monoperiodic, ribbon-like coordination polymer formed, parallel to [010] is built from two strands of uranyl isophthalate linked through oblique, central L ligands, the chain in projection along its axis having overall the same S-shape as L. The connectivity in the polymer is similar to that found in the mixed-

ligand complex of uranyl ion with isophthalate and the aliphatic zwitterion *N,N,N′,N′*-tetramethylethane-1,2-diammonioacetate,[30] but the chain has a considerably thicker profile when regarded along its axis. With a Kitaigorodski packing index (KPI) of 0.72, the packing is quite compact and it involves interchain, parallel-displaced π-stacking interactions between $ipht^{2-}$ anions [centroid···centroid distance, 3.6295(11) Å; dihedral angle, 0°], resulting in the formation of thick layers parallel to (100). Interactions of the zwitterions apart from their coordination are largely of the CH···O type and involve both aliphatic and aromatic hydrogen atoms.

The same uranium coordination mode is found in the complex $[(UO_2)_2(L)(1,2\text{-}pda)_2]\cdot 2H_2O$ (**2**) [U–O(oxo), 1.7679(18) and 1.7773(19) Å; U–O(carboxylato), 2.426(2)–2.521(2) Å], but here the shapes of the ligands are different, with the centrosymmetric L adopting an extended, quasi-linear conformation while $1,2\text{-}pda^{2-}$ has pseudo-twofold rotation symmetry, one carboxylate group oriented away from each side of the ring (Figure 2). The ribbon-like monoperiodic coordination polymer formed runs along [100] and is wider than that in **1**, with the uranium centers linked by L being 19.0740(4) Å apart, compared to 12.4477(3) Å in **1**, the overall width of the ribbon being ~29 Å, compared to ~14 Å in **1**. Interchain, parallel-displaced π-stacking interactions between $1,2\text{-}pda^{2-}$ and L [centroid···centroid distance, 3.9705(18) Å; dihedral angle, 15.83(15)°] generate tightly packed layers (KPI, 0.73) parallel to (01$\bar{1}$). The water molecule forms two hydrogen bonds with carboxylate oxygen atoms from both ligands in the same chain, thus giving a ring with the $R_2^2(13)$ graph set descriptor.[57]

Substituting $1,3\text{-}pda^{2-}$ for $1,2\text{-}pda^{2-}$ has a dramatic and unexpected effect on the structure. The two independent uranium atoms in $[(UO_2)_2(L)(1,3\text{-}pda)_2]\cdot 0.5CH_3CN$ (**3**) are in coordination environments similar to those in **1** and **2**, being κ^2O,O'-chelated by one L and two $1,3\text{-}pda^{2-}$ ligands [U–O(oxo), 1.753(6)–1.779(5) Å; U–O(carboxylato), 2.416(5)–2.525(5) Å] (Figure 3). However, all three ligands are here convergent and C-shaped. The bipyridine unit is

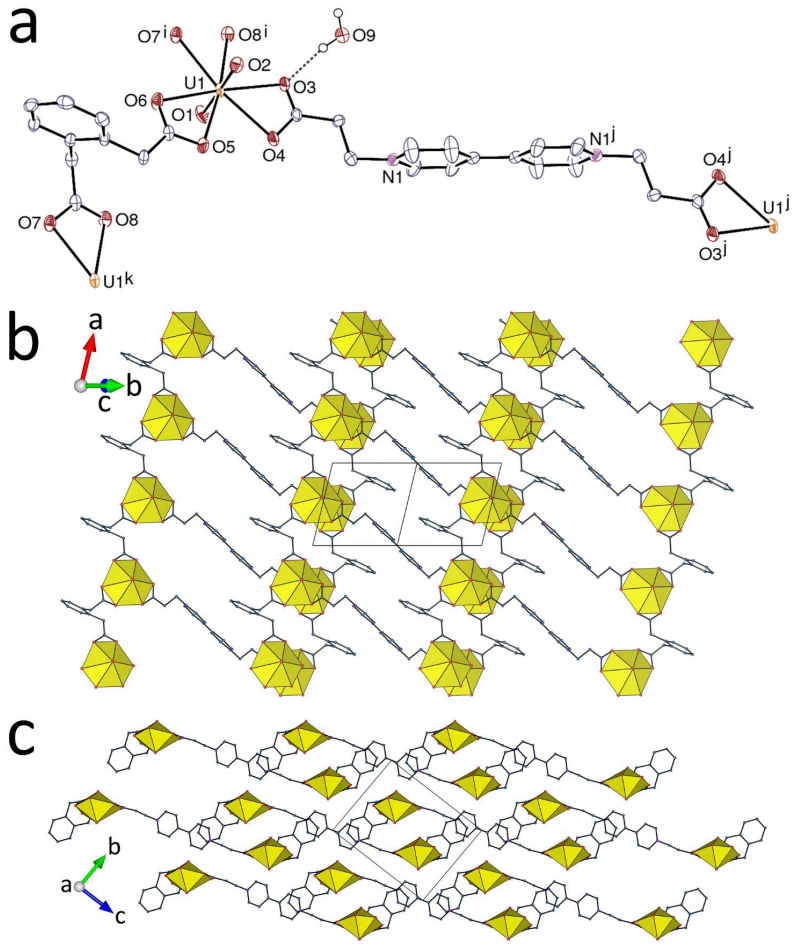

Figure 2. (a) View of compound **2**. Displacement ellipsoids are drawn at the 50% probability level. Carbon-bound hydrogen atoms are omitted and the hydrogen bond is shown as a dashed line. Symmetry codes: i = *x* – 1, *y*, *z*; j = –*x*, 2 – *y*, 2 – *z*; k = *x* + 1, *y*, *z*. (b) Arrangement of chains in a layer. (c) Packing with chains viewed end-on.

no longer planar, the two aromatic rings making a dihedral angle of 38.5(3)° and, more remarkably, the two carboxylate groups are distinctly convergent, resulting in a U1···U2 distance of only 7.2939(5) Å which is suitable for bridging by the smaller 1,3-pda^{2-} ligands, also in a convergent conformation, if accompanied by a tilting of the uranyl equatorial planes with respect to one another [dihedral angle, 59.42(11)°]. The asymmetric, neutral molecular cage thus formed is chiral, thus making **3** a new member of the family of uranyl-based helicates,[13] but it crystallizes as a racemate in a centrosymmetric space group. Viewed down

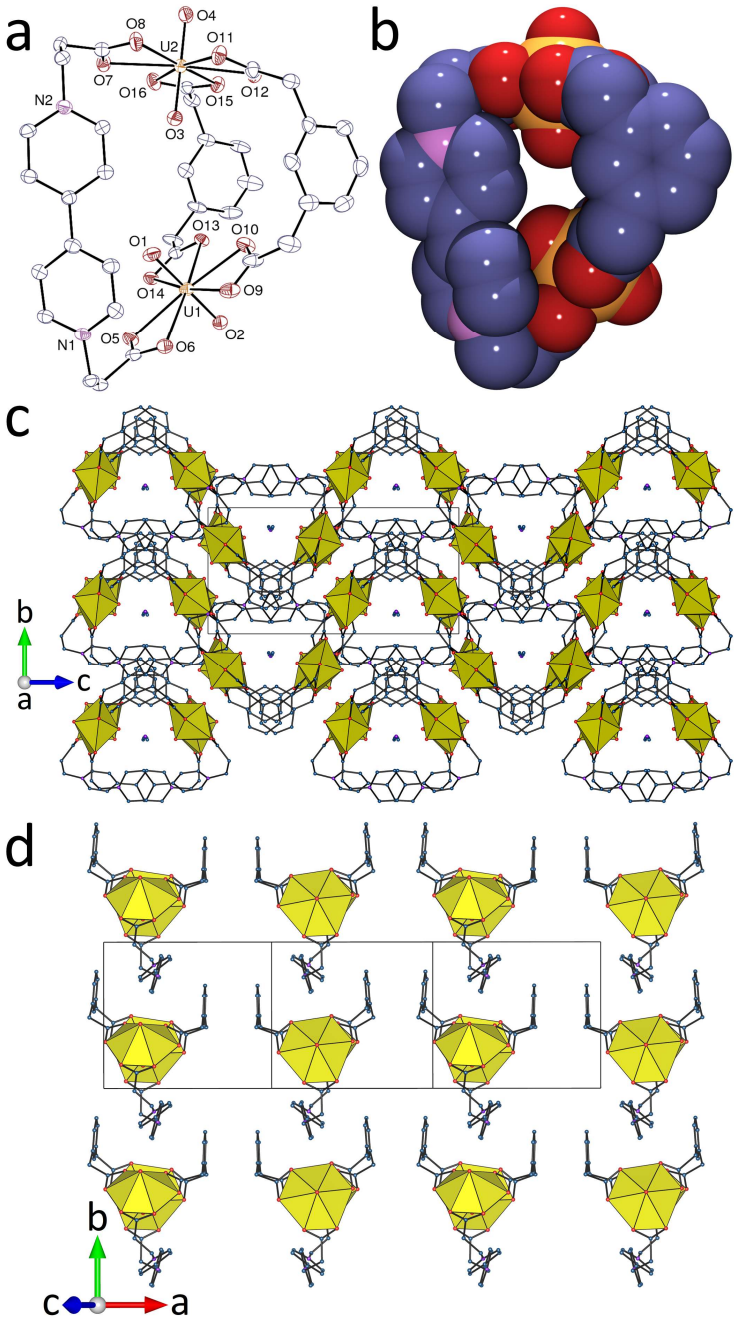

Figure 3. (a) View of compound **3**. Displacement ellipsoids are drawn at the 30% probability level and hydrogen atoms are omitted. (b) Space-filling representation of the cage (U, yellow; O, red; N, purple; C, blue). (c) View of the packing. (d) View of a single layer of homochiral columns.

[100], the array of molecules defines channels occupied by disordered acetonitrile molecules which are directed toward the cage entrance (Figure 3c). Along a given channel composed of a column of similarly oriented molecules, the chirality of the molecules alternates but the

structure also involves columns along [010] in which the two 1,3-pda^{2-} phenyl groups act as a pincer to envelop the bipyridine of the next molecule (Figure 3d) and these columns are homochiral. This arrangement is accompanied by parallel-displaced π-stacking interactions between 1,3-pda^{2-} and L in adjacent molecules along the column axis [centroid···centroid distance, 3.837(6) Å; dihedral angle, 14.0(5)°], while others are between 1,3-pda^{2-} anions in neighbouring columns. However, the most conspicuous interactions are CH···O hydrogen bonds involving other cages and acetonitrile molecules (the latter associated with the uranyl oxo groups located inside the cage), as shown by the Hirshfeld surface (HS) and its associated fingerprint plot (Figure 4). Overall, the CH···O hydrogen bonds represent 43.7% of the HS and H···H interactions represent 35.3%.

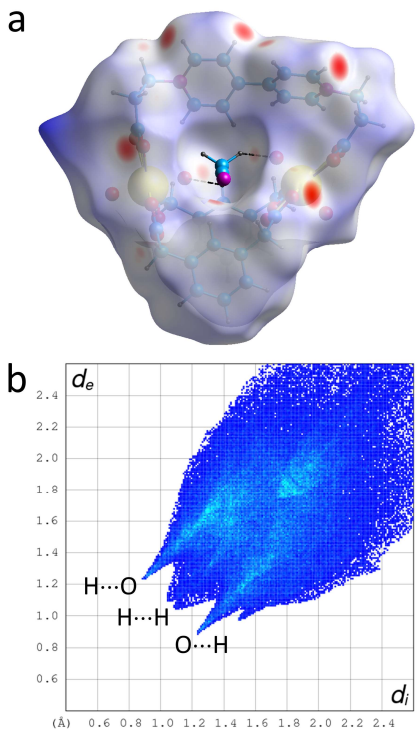

Figure 4. (a) Hirshfeld surface (HS) of complex **3** mapped with d_{norm}. The possible CH···O interactions involving CH_3CN are shown as dashed lines. The red dots on the HS correspond to CH···O interactions with neighbouring cages. (b) Associated fingerprint plot. The nature of the interactions associated with the main features is indicated with the atom located inside the HS first.

The complex $[(UO_2)_2(L)(1,4\text{-pda})(1,4\text{-pdaH})_2]$ (**4**) differs from **1**–**3** by having a different stoichiometry, with a metal/L/anionic ligand ratio of 2:1:3 instead of 2:1:2 in the three other cases, which composition is due to the presence in the asymmetric unit of one centrosymmetric, fully deprotonated anionic ligand and one only half-deprotonated. Here also, the uranium atom is tris(κ^2O,O'-chelated) by one L and two 1,4-pda^{2-}/1,4-pdaH$^-$ ligands [U–O(oxo), 1.769(3) and 1.788(3) Å; U–O(carboxylato), 2.430(4)–2.510(4) Å] (Figure 5). The

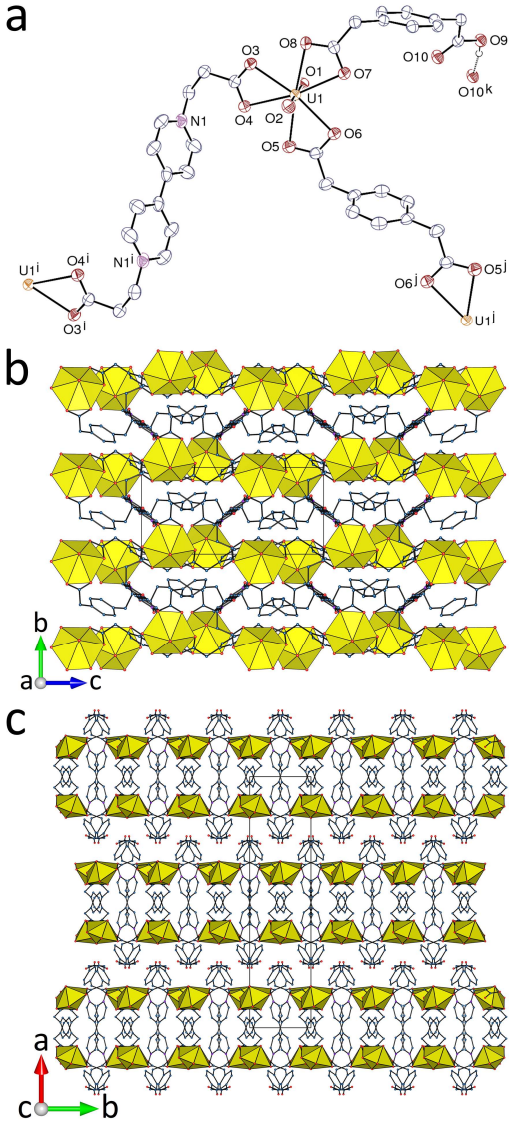

Figure 5. (a) View of compound **4**. Displacement ellipsoids are drawn at the 50% probability level. Carbon-bound hydrogen atoms are omitted and the hydrogen bond is shown as a dashed line. Symmetry codes: i = 1 – *x*, 2 – *y*, 1 – *z*; j = 1 – *x*, 1 – *y*, 2 – *z*; k = 1/2 – *x*, 1/2 – *y*, 2 – *z*. (b) View of one layer of woven chains. (c) Packing with layers viewed edge-on.

1,4-pdaH$^-$ ligand being only bound through the carboxylic group and thus terminal, the monoperiodic coordination polymer formed is a very sinuous, simple chain with the uncoordinated carboxylic groups directed sideways (Figure 6a). Two families of chains run parallel to one another along the [01$\bar{1}$] and [011] directions, the shape of the chains unexpectedly allowing weaving of the two families (Figures 5b and 6b). The motif thus obtained corresponds

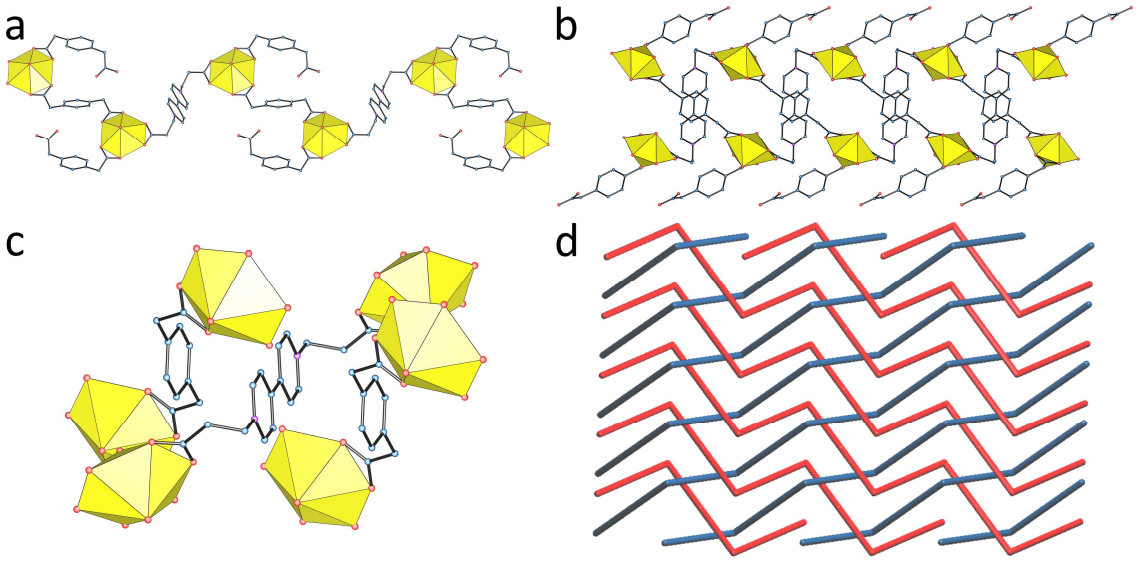

Figure 6. (a) View of one chain in **4**. (b) Woven chains within a layer. (c) View of the π-stacking at the crossing point between the chains. (d) Simplified view of one layer of woven chains.

to the simplest, plain weave, diaxial structure, as shown in Figure 6d, with however an angle between weft and warp of 49° instead of the usual 90° of the **sql-w** weaving pattern[58,59] (and in fact closer to the angle of 60° found in triaxial weaving). The woven chains are arranged in thick layers (~18 Å) parallel to (100), the 1,4-pdaH$^-$ ligands being directed outward on either side (Figure 5c). Within the layers, the crossing points between chains correspond to stacks of aromatic rings of the L and 1,4-pda^{2-} ligands along [010], with however no significant π-stacking interaction [centroid···centroid distance, 4.054(3) Å], while CH···π interactions involve

the methylene groups of 1,4-pda^{2-} and L [H···centroid distance, 2.91 Å; C–H···centroid angle, 141°] (Figure 6c). In previous work, aromatic interactions have been found to play an essential role in the self-assembly of woven organic threads,[36] in the same way as metal cation templates in the more usual weaving strategies based on metal ion coordination.[34,35,37–40,60] The carboxylic groups protruding on both sides of the layers are involved in reciprocal hydrogen bonding [O···O distance, 2.662(5) Å; O–H···O angle, 173(6)°]. These hydrogen bonds link threads pertaining to different layers to form two families of weakly bonded diperiodic networks with the **hcb** topology, parallel to either $(1\bar{1}\bar{1})$ or $(11\bar{1})$, which are involved in inclined 2D + 2D → 3D polycatenation with [101] as zone axis and a dihedral angle of 49° between the intersecting layers, each hexanuclear ring being crossed by three links (Figure 7). The diperiodic woven coordination polymer is thus part of a hydrogen bonded polycatenated assembly of higher periodicity. Some small voids in the structure (KPI, 0.69) are probably occupied by one disordered water molecule (see Experimental Section).

The complex $[(UO_2)_4(LH)_2(1,4\text{-pda})_5]\cdot H_2O\cdot 2CH_3CN$ (**5**) resulted from an attempt to include two zwitterions within the same complex using a mixture of 1,4-pdaH_2, LH_2Cl_2 and *N,N,N′,N′*-tetramethylpropane-1,3-diammonioacetate hydrochloride, the latter having previously been successfully used to synthesize mixed-ligand uranyl ion complexes.[30] Although L is the only zwitterion eventually present in the final compound, the structure of **5** is very different from that of **4**. The two independent uranyl cations are both tris(κ^2*O,O′*)-chelated, U1 by three 1,4-pda^{2-} ligands and U2 by two 1,4-pda^{2-} and one LH$^+$ [U–O(oxo), 1.769(4)–1.770(5) Å; U–O(carboxylato), 2.435(5)–2.508(5) Å] (Figure 8). The main difference with all other complexes is that LH$^+$ is here a terminal ligand, with the uncoordinated carboxylic group retaining its proton. The three independent 1,4-pda^{2-} ligands, one of them centrosymmetric,

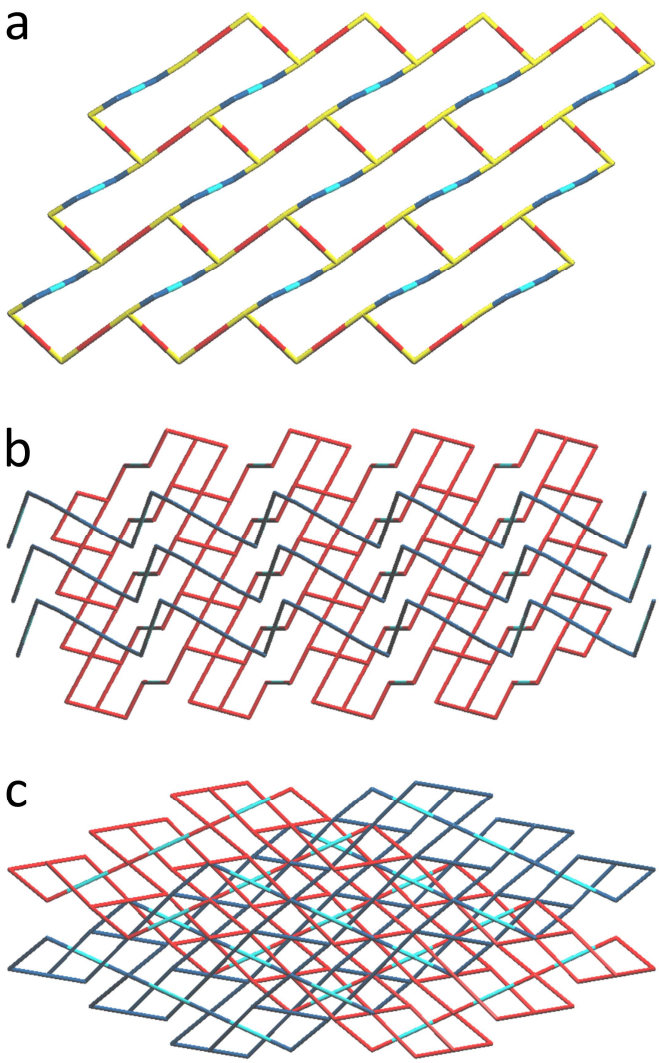

Figure 7. (a) Simplified view of one hydrogen-bonded layer in **4** (uranium, yellow; bridging ligands, red; hydrogen bonded ligand, dark blue; hydrogen bond, light blue). (b) and (c) Simplified views of the polycatenated networks down [001] or down the zone axis [101], respectively. The hydrogen bond links are shown in light blue for both the dark blue and red networks.

have different conformations; one, containing atoms O5–O8, is *cis* and C-shaped, another, containing atoms O9–O12 has one carboxylate group nearly straddling the aromatic mean plane, and the centrosymmetric one, containing atoms O13 and O14, is *trans* and S-shaped. The coordination polymer formed by the 1,4-pda^{2-} ligands is monoperiodic and parallel to [010]. It is based on very elongated tetranuclear rings (smaller and larger distances of 5.8 and 21.5 Å

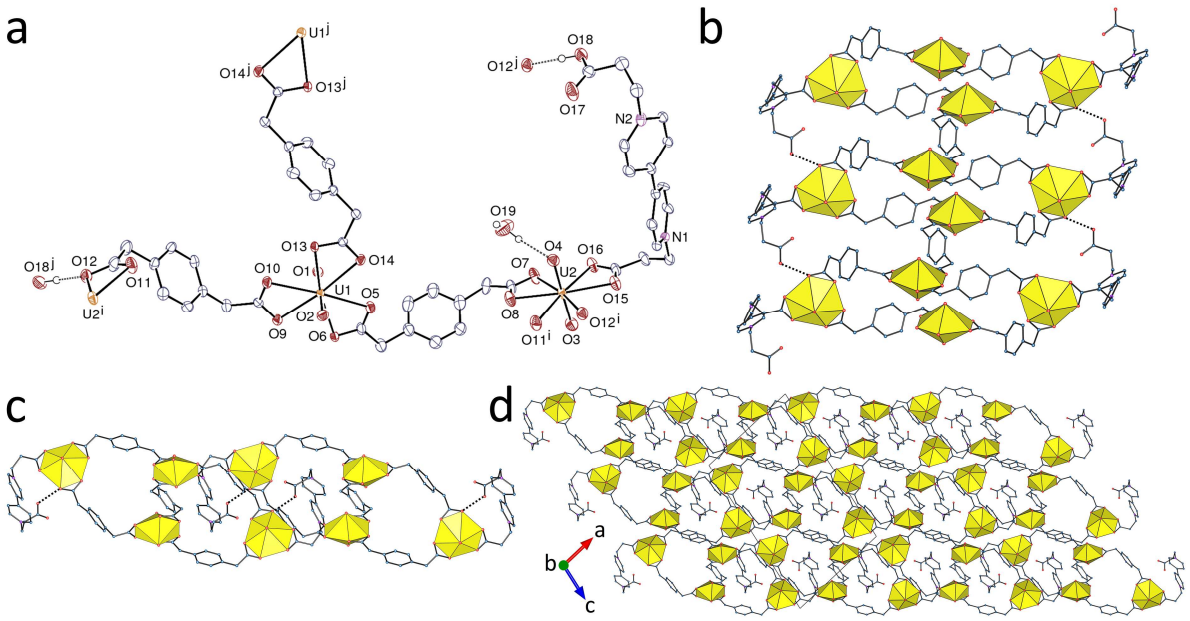

Figure 8. (a) View of compound **5**. Displacement ellipsoids are drawn at the 50% probability level. Carbon-bound hydrogen atoms are omitted and hydrogen bonds are shown as dashed lines. Symmetry codes: i = 1 – *x*, 1 – *y*, –*z*; j = 1 – *x*, –*y*, –*z*. (b) Oblique view of one ring-based chain with hydrogen bonds shown as dotted lines. (c) End-on view of two associated chains. (d) Packing with chains viewed end-on.

between uranium atoms) connected to one another by the centrosymmetric bridge, thus giving an alternation of rings and rods (Figure 8b). This arrangement is somewhat reminiscent of the tubelike coordination polymers formed by the phenylenediacetate ligands,[61] although here the bridging centrosymmetric ligand is located on the chain main axis and thus obstructs the central cavity. The LH^+ cationic ligands are projected sideways on both sides of the rings, and their convergent, C-shaped conformation (close to that in **3**) allows for intrachain hydrogen bond formation with the carboxylate atom O12 [O···O distance, 2.623(7) Å; O–H···O angle, 172(8)°], thus forming a second series of rings, here also tetranuclear but involving LH^+ in place of one 1,4-pda^{2-} ligand, and with each of the $(UO_2)_4$(1,4-pda)$_4$ coordination rings being surrounded by four hydrogen bond-containing rings (Figure 8b). This arrangement has an interesting consequence in that each hydrogen bond-containing link crosses a tetranuclear $(UO_2)_4$(1,4-

pda)$_4$ ring pertaining to an adjoining chain (Figure 9), resulting in the formation of a diperiodic assembly parallel to (10–2) through parallel 1D + 1D → 2D polycatenation.[62] This arrangement is akin to that found in polyrotaxanes,[63,64] although with the difference that the rings here are not 2-membered and each one bears two LH^+ rods and is crossed by two such rods from neighbouring chains. As in complex **4**, the association of polymeric units involves parallel-displaced π-stacking interactions within stacks of 1,4-pda^{2-} and LH^+ [centroid···centroid distances, 3.928(4)–4.266(4) Å; dihedral angles, 8.7(3)–23.6(3)°]. The packing is quite compact (KPI, 0.71), but no interlayer aromatic interactions are present.

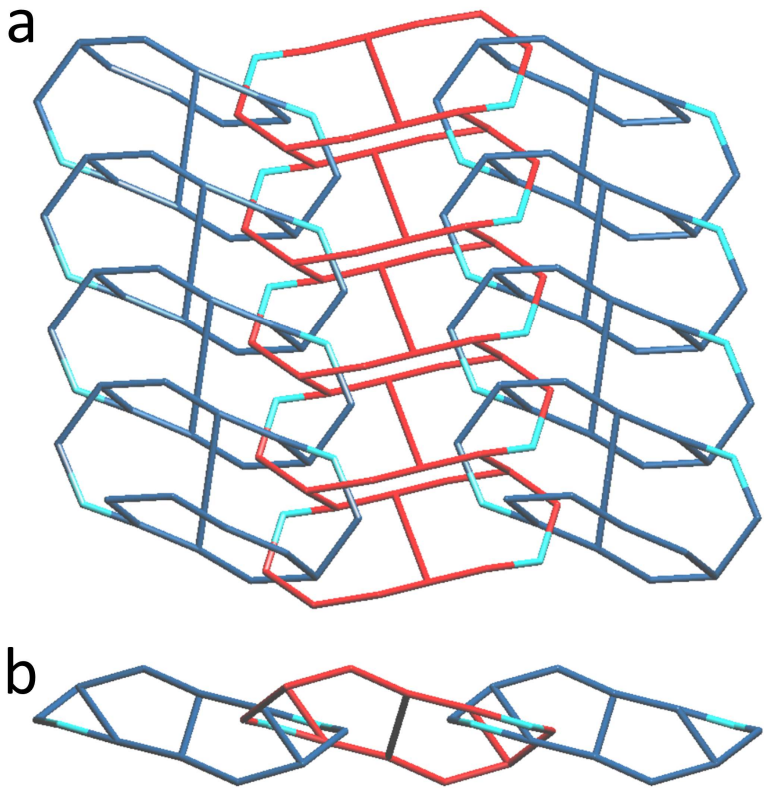

Figure 9. Oblique (a) and edge-on (b) simplified views of the polycatenated chains in **5**. The hydrogen bond links are shown in light blue for both the dark blue and red chains.

Although the ligands used in this series of complexes are only moderately flexible, the geometric variations affecting curvature appear to be large enough to allow the isolation of complexes with very different structures. The conformations of the zwitterionic and anionic

dicarboxylate couples in **1**–**4** are shown in Figure 10 (LH^+ has no uranyl-bridging role in **5**, and its shape is analogous to that in **3**). The L molecule is centrosymmetric in all complexes but **3** (and **5**), and the dihedral angle between the aromatic rings of 38.5(3)° in **3** introduces only a

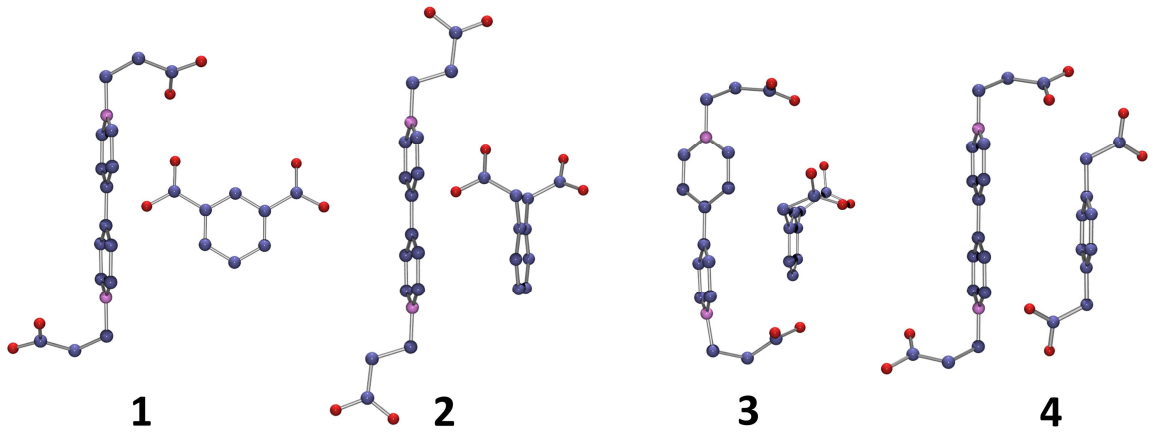

Figure 10. Conformation of the zwitterionic and anionic bridging dicarboxylate couples in complexes **1**–**4**.

minor twist, so that the bipyridine unit in itself may be considered as merely a spacer with little influence on the periodicity of the structure, though of course it does introduce an element of chirality in complex **3**. Three conformations of the carboxylatoethyl arms are found, kinked and located on different sides of the bipyridine unit (**1** and **4**), kinked on the same side (**3** and **5**), and extended (**2**). Obviously, all forms of L but that found in **3** and **5** result in a divergent linker promoting the formation of polymeric species. The anionic ligands found in **1** and **2** are extremely close to one another with respect to the location of the carboxylate groups, with only a larger separation in $ipht^{2-}$ than in 1,2-pda^{2-}. The twofold rotational symmetry or pseudo-symmetry of 1,2-pda^{2-}, as found here, is by far the most common in the complexes formed by this anion, notably with uranyl,[61,65–67] so that no unusual conformation results from its combination with L. Both the *trans*, S-shaped and *cis*, C-shaped conformations of 1,3-pda^{2-} and 1,4-pda^{2-} are frequently found in uranyl ions complexes,[61,65–68] and they often coexist in the same species, as here in **4**, in which the bridging ligand is S-shaped and the terminal, mono-protonated one (not shown in Figure 10) is C-shaped. The C-shaped form of 1,4-pda^{2-} would

seem to be as well adapted as that of 1,3-pda^{2-} to form a cage species, and with a better match between the lengths of the anionic and zwitterionic ligands, so that the difference in structure and the presence of a half-deprotonated ligand in **4** can only be ascribed to the subtle balance between the various forces such as coordination preferences, hydrogen bonding and aromatic interactions, for example, determining the solubility of a given crystalline species. In this respect, the building of a woven structure in **4**, although not completely surprising, can only be rationalized in such very general terms. Moreover, it should be noted that this structure is obtained in the crystalline state only, with no separation of the woven layers as free-standing units, as possible in other cases in which weaving results from a deliberate strategy.[35–38] As in previous studies with uranyl[61,65,66] as well as transition metal cations,[69,70] the conformational flexibility and variable separation between complexing sites of the phenylenediacetate isomers proves in the present series to be a rich source of widely different, novel structures. Complex **5** is somewhat apart from the four other species since it involves monoprotonated, terminal LH^+ ligands, and the monoperiodic polymer formed pertains to the family of uranyl phenylenediacetate coordination polymers. However, the convergent conformation of the pendent LH^+ cations allows the formation of intrachain hydrogen bonded rings and results in polycatenation involving LH^+ rods, so that both ligands play different but equally structure-determining roles.

Luminescence Properties. Complexes **1**–**3** and **5** are significantly emissive in the solid state at room temperature under excitation at 420 nm (Figure 11). Complex **2** exhibits a high photoluminescence quantum yield (PLQY) of 19%, while those for **1**, **3** and **5** are smaller, at 2, 9 and 4%, respectively. In contrast, complex **4** is weakly emissive, with a PLQY lower than 1%. The PLQY values roughly correlate with the minimum U···U distances in the structures [6.7126(2) Å in **1**, 5.5679(2) Å in **2**, 6.6336(6) Å in **3**, 7.8259(5) Å in **4**, and 5.8420(5) Å in **5**] but, as we have discussed previously,[24] this does not appear in general to be a reliable predictor

of PLQY values. The spectra of **1**–**3** and **5** display the vibronic fine structure typical of uranyl ion,[71,72] with maxima at 463–468, 481–484, 501–505, 517–527, 546–552, and 572–578 nm. Two peaks in the spectrum of **3** are split into two components, possibly due to the somewhat different second-sphere environment of the two uranium atoms. These values match those usual for complexes with tris(κ^2*O*,*O*′)-chelated uranyl ions.[73]

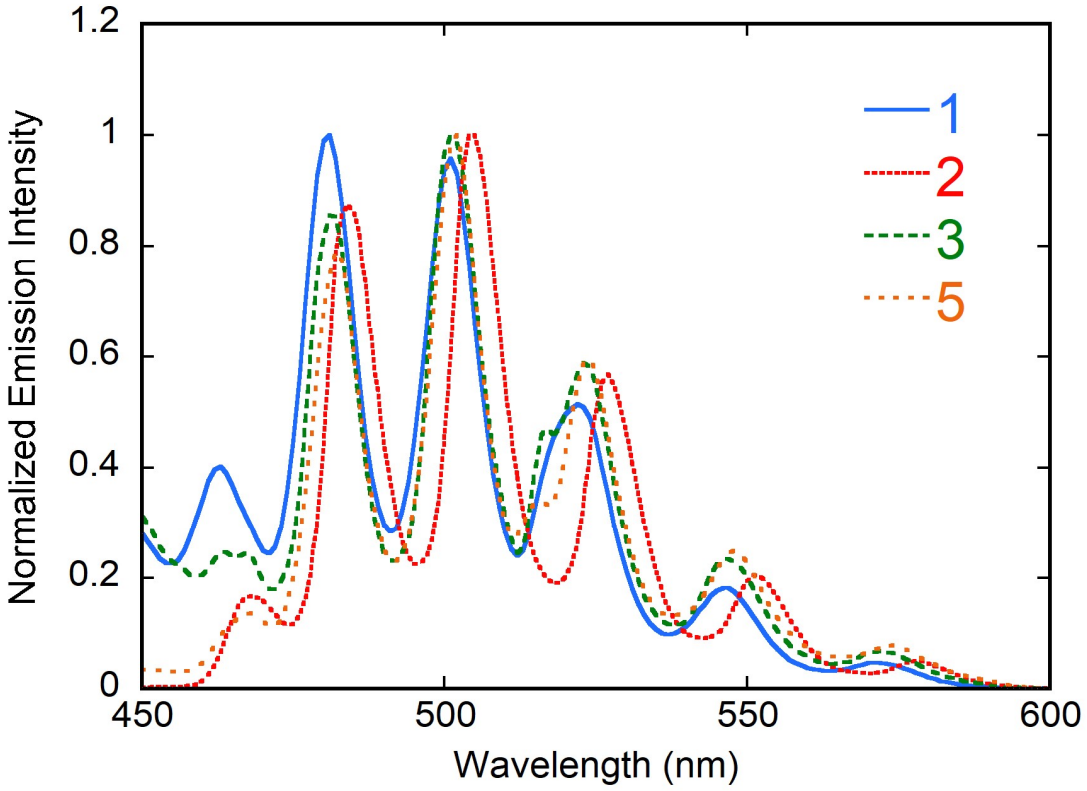

Figure 11. Emission spectra of compounds **1**–**3** and **5** in the solid state at room temperature, under excitation at a wavelength of 420 nm.

CONCLUSIONS

We have reported here the synthesis, crystal structure and luminescence properties of five heteroleptic uranyl ion complexes involving mixtures of one zwitterionic with four different anionic dicarboxylates. Both the zwitterion L and the three positional isomers of phenylenediacetate are conformationally flexible, while isophthalate is much less so. In three of the five complexes, L assumes a divergent geometry, either extended or kinked at both ends,

and its association with the divergent linkers ipht^{2-}, *trans*-1,2-pda^{2-} and *trans*-1,4-pda^{2-} results in the formation of monoperiodic polymers, which are either ribbon-like and two-stranded with L as a central linker (complexes **1** and **2** with ipht^{2-} and 1,2-pda^{2-}, respectively), thread-like and meandering (complex **4** with 1,4-pda^{2-}), or based on an alternation of rods and tetranuclear rings with terminal LH^{+} ligands (complex **5** with 1,4-pda^{2-}). Complex **4** provides an example of the plain weave topology of differently oriented threads, with further formation of hydrogen bonded diperiodic networks involved in inclined polycatenation, and complex **5** displays parallel polycatenation of monoperiodic polymers. It is only in complex **3** that both L and the anionic ligand *cis*-1,3-pda^{2-} adopt convergent geometries, and the resulting discrete, binuclear complex is the first heteroleptic uranyl carboxylate coordination cage. In contrast to known binuclear, anionic triple-stranded uranyl helicates[13] involving three identical dicarboxylate ligands, the mixture of one neutral and two anionic ligands in **3** provides easy access to a neutral cage, an approach which should be exploitable with other zwitterionic carboxylates.

Acknowledgements: This work was supported by Iketani Science and Technology Foundation, and KAKENHI Grant-in-Aid for Early-Career Scientists JP22K14698 for S. Kusumoto, and Thammasat University Research Fund, Contract No. TUFF02/2565 for K. Chainok.

ASSOCIATED CONTENT

Accession Codes

CCDC 2237557−2237560 and 2238390 contain the supplementary crystallographic data for this paper. These data can be obtained free of charge via www.ccdc.cam.ac.uk/data_request/cif, or by emailing data_request@ccdc.cam.ac.uk, or by contacting The Cambridge

Crystallographic Data Centre, 12 Union Road, Cambridge CB2 1EZ, UK; fax: +44 1223 336033.

Supporting Information

The Supporting Information is available free of charge at . Figure S1: ^{1}H NMR spectrum of LH_2Cl_2. (PDF).

AUTHOR INFORMATION

Corresponding Authors

*E-mail: kc@tu.ac.th (K. C.)

*E-mail: ykim@kumamoto-u.ac.jp (Y.K.)

*E-mail: harrowfield@unistra.fr (J.H.)

*E-mail: pierre.thuery@cea.fr (P.T.)

ORCID

Sotaro Kusumoto: 0000-0002-7501-383X

Youssef Atoini: 0000-0003-4851-3713

Kittipong Chainok: 0000-0003-1486-9164

Yang Kim: 0000-0001-8187-0793

Jack Harrowfield: 0000-0003-4005-740X

Pierre Thuéry: 0000-0003-1683-570X

Notes

The authors declare no competing financial interest.

REFERENCES

1. Pullen, S.; Clever, G. H. Mixed-Ligand Metal–Organic Frameworks and Heteroleptic Coordination Cages as Multifunctional Scaffolds–A Comparison. *Acc. Chem. Res*. **2018**, *51*, 3052–3064.
2. Bloch, W. M.; Clever, G. H. Integrative Self-Sorting of Coordination Cages Based on 'Naked' Metal Ions. *Chem. Commun*. **2017**, *53*, 8506–8516.
3. Zheng, Y. R.; Zhao, Z.; Wang, M.; Ghosh, K.; Pollock, J. B.; Cook, T. R.; Stang, P. J. A Facile Approach toward Multicomponent Supramolecular Structures: Selective Self-Assembly via Charge Separation. *J. Am. Chem. Soc*. **2010**, *132*, 16873–16882.
4. Thuéry, P.; Nierlich, M.; Baldwin, B. W.; Komatsuzaki, N.; Hirose, T. A Metal-Organic Molecular Box Obtained from Self-Assembling around Uranyl Ions. *J. Chem. Soc*., *Dalton Trans*., **1999**, 1047–1048.
5. Thuéry, P. A Nanosized Uranyl Camphorate Cage and its Use as a Building Unit in a Metal-Organic Framework. *Cryst. Growth Des*. **2009**, *9*, 4592–4594.
6. Ling, J.; Wallace, C. M.; Szymanowski, J. E. S.; Burns, P. C. Hybrid Uranium–Oxalate Fullerene Topology Cage Clusters. *Angew. Chem. Int. Ed.* **2010**, *49*, 7271–7273.
7. Unruh, D. K.; Ling, J.; Qiu, J.; Pressprich, L.; Baranay, M.; Ward, M.; Burns, P. C. Complex Nanoscale Cage Clusters Built from Uranyl Polyhedra and Phosphate Tetrahedra. *Inorg. Chem.* **2011**, *50*, 5509−5516.
8. Pasquale, S.; Sattin, S.; Escudero-Adán, E. C.; Martínez-Belmonte, M.; de Mendoza, J. Giant Regular Polyhedra from Calixarene Carboxylates and Uranyl. *Nature Commun*. **2012**, *3*, 785–791.
9. Ling, J. Qiu, J.; Burns, P. C. Uranyl Peroxide Oxalate Cage and Core–Shell Clusters Containing 50 and 120 Uranyl Ions. *Inorg. Chem.* **2012**, *51*, 2403−2408.

10. Qiu, J.; Burns, P. C. Clusters of Actinides with Oxide, Peroxide, or Hydroxide Bridges. *Chem. Rev.* **2013**, *113*, 1097–1120.
11. Thuéry, P. A Highly Adjustable Coordination System: Nanotubular and Molecular Cage Species in Uranyl Ion Complexes with Kemp's Triacid. *Cryst. Growth Des*. **2014**, *14*, 901–904.
12. Thuéry, P. Increasing Complexity in the Uranyl Ion–Kemp's Triacid System: From One- and Two-Dimensional Polymers to Uranyl–Copper(II) Dodeca- and Hexadecanuclear Species. *Cryst. Growth Des.* **2014**, *14*, 2665–2676.
13. Thuéry, P.; Harrowfield, J. A New Form of Triple-Stranded Helicate Found in Uranyl Complexes of Aliphatic *α,ω*-Dicarboxylates. *Inorg. Chem.* **2015**, *54*, 10539–10541.
14. Oliveri, A. F.; Pilgrim, C. D.; Qiu, J.; Colla, C. A.; Burns, P. C.; Casey, W. H. Dynamic Phosphonic Bridges in Aqueous Uranyl Clusters. *Eur. J. Inorg. Chem*. **2016**, 797–801.
15. Dembowski, M.; Olds, T. A.; Pellegrini, K. L.; Hoffmann, C.; Wang, X.; Hickam, S.; He, J.; Oliver, A. G.; Burns, P. C. Solution ^{31}P NMR Study of the Acid-Catalyzed Formation of a Highly Charged {$U_{24}Pp_{12}$} Nanocluster, $[(UO_2)_{24}(O_2)_{24}(P_2O_7)_{12}]^{48-}$, and Its Structural Characterization in the Solid State Using Single-Crystal Neutron Diffraction. *J. Am. Chem. Soc.* **2016**, *138*, 8547−8553.
16. Hickam, S.; Burns, P. C. Oxo Clusters of 5*f* Elements. *Struct. Bonding (Berlin, Ger.)* **2017**, *173*, 121−154.
17. Thuéry, P.; Harrowfield, J. Coordination Polymers and Cage-Containing Frameworks in Uranyl Ion Complexes with *rac*- and (1*R*,2*R*)-*trans*-1,2-Cyclohexanedicarboxylates: Consequences of Chirality. *Inorg. Chem.* **2017**, *56*, 1455−1469.
18. Qiu, J.; Spano, T. L.; Dembowski, M.; Kokot, A. M.; Szymanowski, J. E. S.; Burns, P. C. Sulfate-Centered Sodium-Icosahedron-Templated Uranyl Peroxide Phosphate Cages with Uranyl Bridged by μ−η^1:η^2 Peroxide. *Inorg. Chem.* **2017**, *56*, 1874–1880.

19. Thuéry, P.; Harrowfield, J. Tetrahedral and Cuboidal Clusters in Complexes of Uranyl and Alkali or Alkaline-Earth Metal Ions with *rac*- and (1*R*,2*R*)-*trans*-1,2-Cyclohexanedicarboxylate. *Cryst. Growth Des*. **2017**, *17*, 2881–2892.
20. Qiu, J.; Dong, S.; Szymanowski, J. E. S.; Dobrowolska, M.; Burns, P. C. Uranyl-Peroxide Clusters Incorporating Iron Trimers and Bridging by Biphosphonate- and Carboxylate-Containing Ligands, *Inorg. Chem.* **2017**, *56*, 3738–3741.
21. Burns, P. C.; Nyman, M. Captivation with Encapsulation: a Dozen Years of Exploring Uranyl Peroxide Capsules. *Dalton Trans.* **2018**, *47*, 5916–5927.
22. Thuéry, P.; Atoini, Y.; Harrowfield, J. Counterion-Controlled Formation of an Octanuclear Uranyl Cage with *cis*-1,2-Cyclohexanedicarboxylate Ligands. *Inorg. Chem.* **2018**, *57*, 6283–6288.
23. Thuéry, P.; Atoini, Y.; Harrowfield, J. Closed Uranyl–Dicarboxylate Oligomers: A Tetranuclear Metallatricycle with Uranyl Bridgeheads and 1,3-Adamantanediacetate Linkers. *Inorg. Chem.* **2018**, *57*, 7932–7939.
24. Thuéry, P.; Atoini, Y.; Harrowfield, J. Chiral Discrete and Polymeric Uranyl Ion Complexes with (1*R*,3*S*)-(+)-Camphorate Ligands: Counterion-Dependent Formation of a Hexanuclear Cage. *Inorg. Chem.* **2019**, *58*, 870-880.
25. Xu, M.; Eckard, P.; Burns, P. C. Organic Functionalization of Uranyl Peroxide Clusters to Impact Solubility. *Inorg. Chem.* **2020**, *59*, 9881–9888.
26. Cheng, L.; Liang, C.; Liu, W.; Wang, Y.; Chen, B.; Zhang, H.; Wang, Y.; Chai, Z.; Wang, S. Three-Dimensional Polycatenation of a Uranium-Based Metal–Organic Cage: Structural Complexity and Radiation Detection. *J. Am. Chem. Soc*. **2020**, *142*, 16218–16222.
27. Thuéry, P.; Harrowfield, J. Cavity Formation in Uranyl Ion Complexes with Kemp's Tricarboxylate: Grooved Diperiodic Nets and Polynuclear Cages. *Inorg. Chem.* **2021**, *60*, 1683–1697.

28. Thuéry, P.; Harrowfield, J. Ni(2,2′:6′,2″-terpyridine-4′-carboxylate)$_2$ Zwitterions and Carboxylate Polyanions in Mixed-Ligand Uranyl Ion Complexes with a Wide Range of Topologies. *Inorg. Chem*. **2022**, *61*, 9725–9745.

29. Kusumoto, S.; Atoini, Y.; Masuda, S.; Kim, J. Y.; Hayami, S.; Kim, Y.; Harrowfield, J.; Thuéry, P. Zwitterionic and Anionic Polycarboxylates as Coligands in Uranyl Ion Complexes, and Their Influence on Periodicity and Topology. *Inorg. Chem.* **2022**, *61*, 15182−15203.

30. Kusumoto, S.; Atoini, Y.; Masuda, S.; Koide, Y.; Kim, J. Y.; Hayami, S.; Kim, Y.; Harrowfield, J.; Thuéry, P. Flexible Aliphatic Diammonioacetates as Zwitterionic Ligands for UO_2^{2+}: Complexes with Diverse Topologies and Interpenetrated Structures. *Inorg. Chem.*, in the press.

31. Li, X. N.; Li, L.; Wang, H. Y.; Fu, C.; Fu, J. W.; Sun, Y. N.; Zhang, H. A Novel Photochromic Metal–Organic Framework with Good Anion and Amine Sensing. *Dalton Trans*. **2019**, *48*, 6558–6563.

32. Li, X. N.; Li, L.; Wang, Z. H.; Wu, G. H.; Liu, S. Q.; Zhang, H. Two Isomeric Cd-Viologen Coordination Polymers with Photochromic and Photoluminescence Properties. *Dyes Pigments* **2021**, *184*, 108800.

33. Zeng, L. W.; Hu, K. Q.; Mei, L.; Li, F. Z.; Huang, Z. W.; An, S. W.; Chai, Z. F.; Shi, W. Q. Structural Diversity of Bipyridinium-Based Uranyl Coordination Polymers: Synthesis, Characterization, and Ion-Exchange Application. *Inorg. Chem*. **2019**, *58*, 14075−14084.

34. Liu, Y.; Ma, Y.; Zhao, Y.; Sun, X.; Gándara, F.; Furukawa, H.; Liu, Z.; Zhu, H.; Zhu, C.; Suenaga, K.; Oleynikov, P.; Alshammari, A. S.; Zhang, X.; Terasaki, O.; Yaghi O. M. Weaving of Organic Threads into a Crystalline Covalent Organic Framework. *Science* **2016**, *351*, 365−369.

35. Wang, Z.; Błaszczyk, A.; Fuhr, O.; Heissler, S.; Wöll, C.; Mayor, M. Molecular Weaving via Surface-Templated Epitaxy of Crystalline Coordination Networks. *Nature Commun*. **2017**, *8*, 14442.

36. Lewandowska, U.; Zajaczkowski, W.; Corra, S.; Tanabe, J.; Borrmann, R.; Benetti, E. M.; Stappert, S.; Watanabe, K.; Ochs, N. A. K.; Schaeublin, R.; Li, C.; Yashima, E.; Pisula, W.; Müllen, K.; Wennemers, H. A Triaxial Supramolecular Weave. *Nature Chem.* **2017**, *9*, 1068−1072.
37. August, D. P.; Dryfe, R. A. W.; Haigh, S. J.; Kent, P. R. C.; Leigh, D. A.; Lemonnier, J. F.; Li, Z.; Muryn, C. A.; Palmer, L. I.; Song, Y.; Whitehead, G. F. S.; Young, R. J. Self-Assembly of a Layered Two-Dimensional Molecularly Woven Fabric. *Nature* **2020**, *588*, 429−435.
38. Li, G.; Wang, L.; Wu, L.; Guo, Z.; Zhao, J.; Liu, Y.; Bai, R.; Yan, X. Woven Polymer Networks via the Topological Transformation of a [2]Catenane. *J. Am. Chem. Soc.* **2020**, *142*, 14343−14349.
39. Leigh, D. A.; Danon, J. J.; Fielden, S. D. P.; Lemonnier, J. F.; Whitehead, G. F. S.; Woltering, S. L. A Molecular Endless (7_4) Knot. *Nature Chem.* **2021**, *13*, 117−122.
40. Jiao, Y.; Stoddart, J. F. Weaving on the Molecular Scale. *Matter* **2021**, *4*, 2582−2584.
41. Sun, C.; Xu, G.; Jiang, X. M.; Wang, G. E.; Guo, P. Y.; Wang, M. S.; Guo, G. C. Design Strategy for Improving Optical and Electrical Properties and Stability of Lead-Halide Semiconductors. *J. Am. Chem. Soc.* **2018**, *140*, 2805−2811.
42. *APEX3 Crystallography Software Suite,* Ver. 2019.1-0; Bruker AXS: Madison, WI, 2019.
43. *SAINT,* Ver. 8.40A; Bruker Nano: Madison, WI, 2019.
44. *SADABS, Bruker/Siemens Area Detector Absorption and Other Corrections,* Ver. 2016/2; Bruker AXS: Madison, WI, 2016.
45. Krause, L.; Herbst-Irmer, R.; Sheldrick, G. M.; Stalke, D. Comparison of Silver and Molybdenum Microfocus X-Ray Sources for Single-Crystal Structure Determination. *J. Appl. Crystallogr.* **2015**, *48,* 3–10.
46. Sheldrick, G. M. SHELXT – Integrated Space-Group and Crystal-Structure Determination. *Acta Crystallogr., Sect. A* **2015**, *71*, 3–8.

47. Sheldrick, G. M. Crystal Structure Refinement with SHELXL. *Acta Crystallogr., Sect. C* **2015**, *71*, 3–8.

48. Hübschle, C. B.; Sheldrick, G. M.; Dittrich, B. *ShelXle*: a Qt Graphical User Interface for SHELXL. *J. Appl. Crystallogr.* **2011**, *44*, 1281–1284.

49. Spek, A. L. *PLATON* SQUEEZE: a Tool for the Calculation of the Disordered Solvent Contribution to the Calculated Structure Factors. *Acta Crystallogr., Sect. C* **2015**, *71*, 9–18.

50. Burnett, M. N.; Johnson, C. K. *ORTEPIII*, Report ORNL-6895; Oak Ridge National Laboratory: TN, 1996.

51. Farrugia, L. J. WinGX and ORTEP for Windows: an Update. *J. Appl. Crystallogr.* **2012**, *45,* 849–854.

52. Momma, K.; Izumi, F. *VESTA* 3 for Three-Dimensional Visualization of Crystal, Volumetric and Morphology Data. *J. Appl. Crystallogr.* **2011**, *44,* 1272–1276.

53. Blatov V. A.; Shevchenko, A. P.; Proserpio, D. M. Applied Topological Analysis of Crystal Structures with the Program Package ToposPro. *Cryst. Growth Des.* **2014**, *14*, 3576–3586.

54. Spek, A. L. Structure Validation in Chemical Crystallography. *Acta Crystallogr., Sect. D* **2009**, *65*, 148–155.

55. Spackman, M. A.; Jayatilaka, D. Hirshfeld Surface Analysis. *CrystEngComm* **2009**, *11*, 19–32.

56. Wolff, S. K.; Grimwood, D. J.; McKinnon, J. J.; Turner, M. J.; Jayatilaka, D.; Spackman, M. A. *CrystalExplorer*, University of Western Australia, 2012.

57. Bernstein, J.; Davis, R. E.; Shimoni, L.; Chang, N. L. Patterns in Hydrogen Bonding: Functionality and Graph Set Analysis in Crystals. *Angew. Chem. Int. Ed.* **1995**, *34*, 1555–1573.

58. Liu, Y.; O'Keeffe, M.; Treacy, M. M. J.; Yaghi, O. M. The Geometry of Periodic Knots, Polycatenanes and Weaving from a Chemical Perspective: a Library for Reticular Chemistry. *Chem. Soc. Rev.* **2018**, *47*, 4642–4664.

59. O'Keeffe, M.; Treacy, M. M. J. Crystallographic Descriptions of Regular 2-Periodic Weavings of Threads, Loops and Nets. *Acta Crystallogr., Sect. A* **2020**, *76*, 110–120.

60. Hubin, T. J.; Busch, D. H. Template Routes to Interlocked Molecular Structures and Orderly Molecular Entanglements. *Coord. Chem. Rev*. **2000**, *200–202*, 5–52.

61. Thuéry, P.; Atoini, Y.; Harrowfield, J. Tubelike Uranyl−Phenylenediacetate Assemblies from Screening of Ligand Isomers and Structure-Directing Counterions. *Inorg. Chem.* **2019** *58*, 6550−6564.

62. Batten, S. R. Interpenetration and Entanglement in Coordination Polymers. In *Metal-Organic Framework Materials, Encyclopedia of Inorganic and Bioinorganic Chemistry*, Eds. L. MacGillivray and C. M. Lukehart, Wiley, Chichester, UK, **2014**, pp. 1–16, DOI: 10.1002/9781119951438.eibc2230.

63. Carlucci, L.; Ciani, G.; Proserpio, D. M. Polycatenation, Polythreading and Polyknotting in Coordination Network Chemistry. *Coord. Chem. Rev.* **2003**, *246*, 247−289.

64. Yang, J.; Ma, J. F.; Batten, S. R. Polyrotaxane Metal−Organic Frameworks (PMOFs). *Chem. Commun.* **2012**, *48*, 7899−7912.

65. Thuéry, P.; Atoini, Y.; Harrowfield, J. 1,2-, 1,3-, and 1,4-Phenylenediacetate Complexes of the Uranyl Ion with Additional Metal Cations and/or Ancillary *N*-Donor Ligands: Confronting Ligand Geometrical Proclivities. *Cryst. Growth Des.* **2019**, *19*, 6611−6626.

66. Thuéry, P.; Atoini, Y.; Harrowfield, J. Structure-Directing Effects of Coordinating Solvents, Ammonium and Phosphonium Counterions in Uranyl Ion Complexes with 1,2-, 1,3-, and 1,4-Phenylenediacetates. *Inorg. Chem.* **2020**, *59*, 2503−2518.

67. Thuéry, P.; Harrowfield, J. Stepwise Introduction of Flexibility into Aromatic Dicarboxylates Forming Uranyl Ion Coordination Polymers: a Comparison of 2-Carboxyphenylacetate and 1,2-Phenylenediacetate. *Eur. J. Inorg. Chem.* **2021**, 2182−2192.

68. Brager, D. M.; Nicholas, A. D.; Schofield, M. H.; Cahill, C. L. Pb−Oxo Interactions in Uranyl Hybrid Materials: A Combined Experimental and Computational Analysis of Bonding and Spectroscopic Properties. *Inorg. Chem.* **2021**, *60*, 17186−17200.

69. Yang, G. P.; Wang, Y. Y.; Zhang, W. H.; Fu, A. Y.; Liu, R. T.; Lermontova, E. K.; Shi, Q. Z. A Series of Zn(II) Coordination Complexes Derived from Isomeric Phenylenediacetic Acid and Dipyridyl Ligands: Syntheses, Crystal Structures, and Characterizations. *CrystEngComm* **2010**, *12*, 1509–1517.

70. Liu, D.; Chang, Y. J.; Lang, J. P. Ligand Geometry-Driven Formation of Different Coordination Polymers from $Zn(NO_3)_2$, 1,4-bpeb and Phenylenediacetic Acids. *CrystEngComm* **2011**, *13*, 1851–1857.

71. Brachmann, A.; Geipel, G.; Bernhard, G.; Nitsche, H. Study of Uranyl(VI) Malonate Complexation by Time Resolved Laser-Induced Fluorescence Spectroscopy (TRLFS). *Radiochim. Acta* **2002**, *90*, 147–153.

72. Demnitz, M.; Hilpmann, S.; Lösch, H.; Bok, F.; Steudtner, R.; Patzschke, M.; Stumpf, T.; Huittinen, N. Temperature-dependent Luminescence Spectroscopic Investigations of Uranyl(VI) Complexation with the Halides F^- and Cl^-. *Dalton Trans*. **2020**, *49*, 7109–7122.

73. Thuéry, P.; Harrowfield, J. Structural Consequences of 1,4-Cyclohexanedicarboxylate Cis/Trans Isomerism in Uranyl Ion Complexes: from Molecular Species to 2D and 3D Entangled Nets. *Inorg. Chem.* **2017**, *56*, 13464−13481.

For Table of Contents Use Only

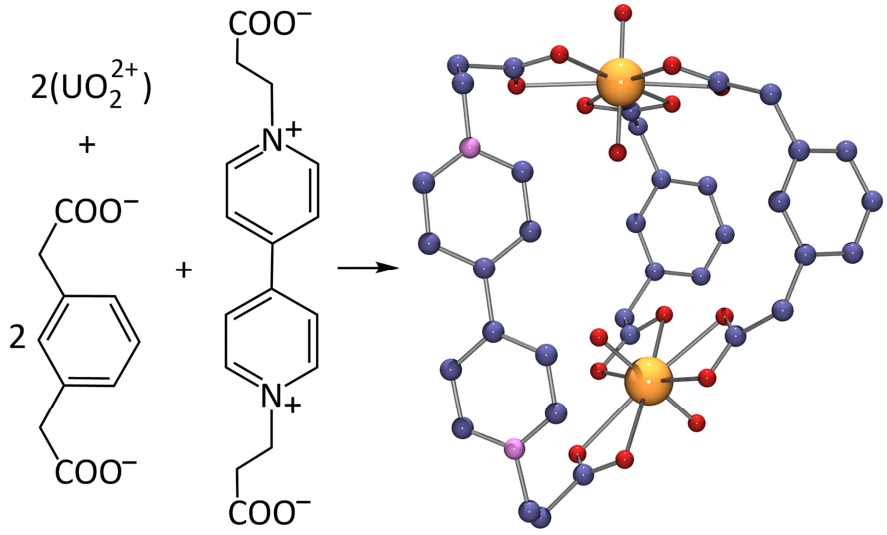

Uranyl ion complexation by mixtures of zwitterionic and anionic dicarboxylate ligands endowed with a range of flexibility and curvature gives two monoperiodic, ribbon-like coordination polymers, a case of polycatenated, ring-containing chains, and unique examples of a heteroleptic, binuclear uranyl polycarboxylate coordination cage and a diperiodic arrangement based on woven uranyl carboxylate chains.